Mobility Shift Affinity Capillary Electrophoresis at High Ligand Concentrations: Application to Aluminum Chlorohydrate–Protein Interactions

Nesrine Ouadah, Claudine Moire, Fabien Brothier, Jean-François Kuntz, Michal Malý, Pavel Dubský, Herve Cottet

ACS OMEGA

Article

Cite This: ACS Omega 2018, 3, 17547−17554

http://pubs.acs.org/journal/acsodf

Mobility Shift Affinity Capillary Electrophoresis at High Ligand Concentrations: Application to Aluminum Chlorohydrate−Protein Interactions

Nesrine Ouadah,[†] Claudine Moire,[‡] Fabien Brothier,[‡] Jean-François Kuntz,[‡] Michal Malý,[§] Pavel Dubský,[§] and Hervé Cottet*[,†]

[†]IBMM, University of Montpellier, CNRS, ENSCM, Montpellier, France

[‡]L'Oréal Research & Innovation, 93600 Aulnay-Sous-Bois, France

[§]Faculty of Science, Department of Physical and Macromolecular Chemistry, Charles University, 128 43 Prague, Czech Republic

Supporting Information

ABSTRACT: The active ingredients in antiperspirant products are aluminum chlorohydrates (ACHs) that, when interacting with proteins present in sweat and sweat duct walls, lead to the obstruction of the sweat ducts and thus reduce delivery of sweat at the skin surface. This study is aimed at developing a methodology based on affinity capillary electrophoresis (ACE) to obtain a quantitative ranking of the interaction between ACHs and proteins under experimental conditions close to those of industrial applications. Usually, in ACE, the metal ligand is introduced at typically μM to mM concentrations in a background electrolyte (BGE) containing a buffering agent that sets the pH and ionic strength. In this work, ACE was implemented in a range of ACH (ligand) concentrations up to 50 g/L (0.2 M in $Al(H_2O)_6{\cdot}3Cl$) in the absence of other buffering agents, to mimic as much as possible the conditions encountered in the production of antiperspirant products. Under such electrophoretic conditions, the challenge is to extract quantitative information about the interaction from the electrophoretic mobility of the protein, knowing that many effects (including Joule heating, viscosity, pH, ionic strength of the BGE, and distribution of the ligands) vary with the concentration of ACH. With relevant corrections on the effective mobility, it has been possible to observe and quantify a much stronger interaction of ACH components with bovine serum albumin compared to lysozyme.

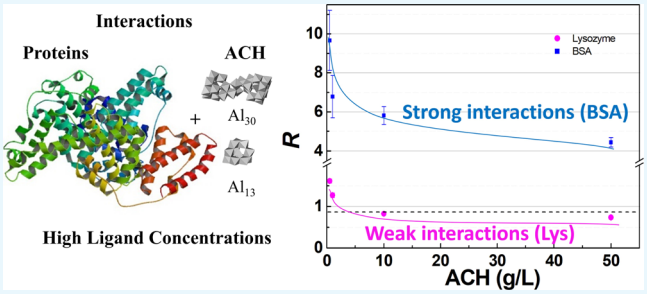

1. INTRODUCTION

Aluminum chlorohydrates (ACHs) and other activated derivatives are the active ingredients in most antiperspirant products.[1−5] Their action in the process of reducing sweating has often been studied at the clinical scale, but little is known on the physicochemical mechanisms involved in sweat reduction. A microfluidic model was recently described[6,7] to study the interactions of ACHs and sweat proteins under controlled realistic conditions. A complexation mechanism between ACH ingredients and sweat proteins leading to the obstruction of the sweat ducts has been brought out, in agreement with in vivo observations.[6,7] However, there is a lack of analytical and biophysical methods allowing characterization and screening of the interactions between ACH ingredients and sweat proteins at a molecular or mesoscopic level.

Among the different analytical techniques used to characterize the ACH oligomers, nuclear magnetic resonance (NMR)[8−10] and size exclusion chromatography[11−13] are probably some of the most important techniques to study structure−activity correlations. More recently, capillary electrophoresis (CE) was found to be very useful for the separation and characterization of different oligomeric forms,[14] including Al_{13}, Al_{30},[1] and other Al hydroxide colloids and aggregated forms of the polycations.[2]

Regarding the study of protein−ACH interactions, Yuan et al.[15] have used zeta potential measurements to evaluate the interactions with bovine serum albumin (BSA), used as a model sweat protein, for predicting the antiperspirant efficacy. ACH−BSA interactions have also been studied using several titration techniques (turbidimetry, potentiometry, and so on),[16,17] and the aggregation of aluminum species has been monitored by scanning electron microscopy (SEM),[16,17] Fourier transform infrared (FTIR) spectroscopy ,[17] dynamic light scattering (DLS),[16] X-ray diffraction,[16] and ^{27}Al solution NMR.[16,17] However, there is still a need to develop alternative and complementary techniques for the quantification and the screening of protein−ACH interactions under conditions close to the conditions of applications.

In CE, interactions can mainly be studied by frontal analysis capillary electrophoresis (FACE), by (mobility shift) affinity

Received: September 10, 2018
Accepted: December 3, 2018
Published: December 17, 2018

DOI: 10.1021/acsomega.8b02326
ACS Omega 2018, 3, 17547−17554

Table 1. Physicochemical Characteristics of the ACH Solutions in Water Used as BGE in ACE[a]

ACH (g/L)	pH	η (10^{-3} mPa·s)	P/L[b] (W/m)	Θ[c]	δT[d] (°C)	i (μA)[e]	I_{eq} (mM)[f]
0.5	4.8	1.07	0.114	0.020	0.3	4.5	8.7
1	4.7	1.11	0.179	0.019	0.5	7.0	12.3
10	4.6	1.15	0.779	0.018	2.2	30.5	45.8
50	4.5	1.34	3.896	0.016	12.7	147.5	213

[a]Experimental conditions: 50 μm i.d. × 38.5 cm, capillary, −10 kV. [b]Dissipated power per capillary length. [c]See eq 8. [d]Difference between the equilibrium temperature and the setpoint temperature (25 °C). [e]Current intensity. [f]Equivalent ionic strength estimated from NaCl solutions giving the same current intensity under the same electrophoretic conditions.

capillary electrophoresis (ACE), or, in a limited number of applications, by direct injection of a ligand/receptor mixture.[18−22] The FACE approach consists of quantifying the free ligand in an equilibrated receptor/ligand mixture and, subsequently, building the isotherm of adsorption to extract the interaction parameters (the binding site interaction constant and the stoichiometry n).[23−27] This approach requires a unique and well-defined couple of receptors/ligands and, hence, can hardly be applied to protein−ACH interactions because ACH solutions are mixtures of several aluminum oligocations with concentration-dependent distributions. In mobility shift ACE, the electrophoretic mobility of the receptor is determined in the BGE containing different concentrations of ligands. A pseudoisotherm of adsorption that can be linearized is thus constructed to extract the binding constants.[28−34] Nevertheless, it should be mentioned that currently, the binding constants are mostly extracted from the adsorption pseudoisotherms by nonlinear regression analysis, which is a preferred and more precise way as compared to the linearized plots, as shown, for example, in ref 35. It is also generally assumed that it is preferable to extract the information about the interaction for the effective electrophoretic mobility after subtraction of the electroosmotic contribution.[28,32] Wätzig's group[36−39] used the normalized difference of the mobility ratios to classify interactions between proteins (BSA, HSA, myoglobulin, and so on) and metals (lithium, sodium, magnesium, calcium, barium, aluminum, gallium, silver, gold, osmium, palladium, platinum, rhodium, ruthenium, iridium, cobalt, copper, nickel, chromium, iron, vanadium, and so on).[39] A similar interaction behavior has been found for aluminum and gallium because of their trivalency. The interaction between BSA and aluminum leads to an increased electrophoretic mobility, explained by the increase in the charge density of the complex Al−BSA. Besides, no other study has reported the investigation of the interactions between ACH and proteins by CE.

The objectives of this study were to explore affinity capillary electrophoresis (ACE) to study protein−ACH interactions at high ligand (ACH) concentrations, compatible with the typical concentration range used in cosmetic antiperspirant products. BSA and lysozyme (LSZ) have been selected as model proteins to mimic sweat proteins and as a matter of comparison with previous studies with other techniques.[16,17] ACH is directly used as a BGE without any other buffering additives to keep the experimental conditions close as much as possible to those of real applications. The analytical challenge, in such a case, is to extract quantitative information regarding the protein−ligand interaction by removing all other undesirable effects that are affecting the electrophoretic mobility of the protein such as Joule heating, viscosity change, ionization state, and ionic strength.[40] It is worth noting that because of the complexity of the oligomeric distribution of ACH mixtures, the aim of this study is to achieve a quantitative ranking of the interaction between ACH and proteins, rather than the direct estimation of the binding constants between protein and a uniquely well-defined ACH oligomer. Ranking the interactions under experimental conditions close to those of industrial applications is a challenging issue that should be addressed, even if the goal is far from the more academic job consisting of determining the binding constant and stoichiometry.

2. EXPERIMENTAL

2.1. Chemicals. 4-Morpholinoethanesulfonic acid (MES), imidazole (Im), and sodium hydroxide (NaOH) were purchased from Acros Organics (NJ, USA). UltraTrol LN was directly acquired from Target Discovery, Inc. (Palo Alto, CA, USA). Ultrapure water was prepared with a Milli-Q system from Millipore (Molsheim, France). The ACH ingredient was provided in a 50% m/v water solution by L'Oréal Laboratories (Aulnay-Sous-Bois, France). BSA and LSZ from chicken egg white were purchased from Aldrich (Milwaukee, WI, USA).

2.2. CE. CE experiments were carried out on a 7100 CE Agilent Technologies system (Waldbronn, Germany) equipped with a diode array detector. A bare fused-silica capillary was purchased from Polymicro Technologies (Phoenix, AZ, USA). The capillary dimensions were 38.5 cm (30 cm to the UV detector) × 50 μm i.d. and 360 μm o.d. The temperature of the capillary cassette was set at 25 °C. The capillary was coated with UltraTrol LN by the following successive flushes at 950 mbar: 2 min with methanol, 2 min with water, 2 min with 1 M NaOH, 3 min with 0.1 M HCl, 3 min with water, 2 min with UltraTrol LN solution, wait for 5 min, and 2 min with water. The coating of the capillary was repeated every 10 analyses. Between runs, the capillary was flushed with BGE for 4 min before each sample injection.

Background electrolyte (BGE) without ACH was prepared by mixing 5 mM NaOH with the desired amount of MES (as indicated in the text) to reach the desired pH, as predicted by PeakMaster.[41] The pH of the BGE was controlled using a Mettler Toledo Seven Compact pH meter (Columbus, OH, USA) before use.

BGE with ACH was prepared by direct dilution of the ACH ingredient in water. No buffering compound was added to the ACH solution to keep the BGE system close as much as possible to those of real-life applications. Table 1 describes the different concentrations of ACH used as BGE for ACE.

The protein sample was prepared by weighing 10 mg of the desired protein (BSA or LSZ) and 2.5 mg of Im as a mobility marker, adjusted to 5 mL in water. The injection volume was set to approximately 1% v/v of the capillary effective volume, that is, 50 mbar and 5 s. Indirect UV detection was recorded at 205 ± 3 nm with a reference at 300 ± 5 nm.

DOI: 10.1021/acsomega.8b02326
ACS Omega 2018, 3, 17547−17554

2.3. Data Treatment. The electrophoretic peaks of BSA and LSZ in the absence or in the presence of ACH are relatively broad because of the inherent heterogeneities of the protein samples. Integration of the peaks on the time-scale electropherograms was operated using CEval 0.6 software[42] to get the average migration time $t_{centroid}$ of the peak (first moment of the peak, which can be different from the migration time at the peak apex). The apparent electrophoretic mobility of the protein was calculated by using eq 1

$$\mu_{app,prot} = \frac{l \times L}{V \times t_{centroid}} \quad (1)$$

where l and L represent the effective and total capillary lengths and V is the applied voltage. The effective electrophoretic mobility was then obtained from eq 2

$$\mu_{ep,prot} = \mu_{app,prot} - \mu_{eo} \quad (2)$$

where μ_{eo} denotes the electroosmotic mobility. μ_{eo} was determined for each electrophoretic run from the electroosmotic perturbation (in the presence of ACH in the BGE), or with the use of an electrophoretic mobility marker (Im, in the absence of ACH in the BGE). The effective (ionic) mobility of the marker (Im) was estimated using PeakMaster software at the same ionic strength as that of the BGE.[41] Each effective mobility value is averaged on $n = 4$ repetitions. In the absence of ACH in the BGE, the effective electrophoretic mobility of the protein is referred to as $\mu_{ep,prot.}$. In the presence of ACH in the BGE, the effective electrophoretic mobility of the protein is referred to as $\mu^*_{ep,prot}$.

To get a clear representation of the mobility distribution, the typical min and max effective mobilities $\mu_{ep,prot}^{min/max}$ were calculated according to eq 3

$$\mu_{ep,prot}^{min/max} = \frac{l \times L}{V(t_{centroid} \mp 2\sigma_{centroid})} - \mu_{eo} \quad (3)$$

where $t_{centroid}$ is the average migration time (which can be different from the peak apex) and $\sigma_{centroid}$ is the electrophoretic migration time standard deviation, both calculated for each peak using a home-customized version of the CEval 0.6 software[42] available at the following address [https://echmet.natur.cuni.cz/software/ceval].

Other corrections due to Joule heating, viscosity, pH, and ionic strength of the BGE were also taken into account and will be further discussed in the Results and Discussion section.

3. RESULTS AND DISCUSSION

To provide a direct comparison of the comparative size of the receptors (proteins) and ligands (ACH) studied in this work, Figure 1 displays a schematic representation, at a constant scale length, of BSA and LSZ proteins and Al_{13} and Al_{30} contained in the ACH solution.

3.1. Noncorrected Electrophoretic Mobility. Figure 2A,B displays the electropherograms of BSA and LSZ, respectively, in X mM MES—5 mM Na BGE (where X varies with pH) in the absence of ACH for different pH values between 4.04 and 4.78 on a neutrally coated capillary in positive polarity (+30 kV). The effective electrophoretic mobility of the proteins was calculated by subtracting the weak EOF contribution using eq 2 (see the CE section). Im was used as a mobility marker, and its ionic electrophoretic mobility was given by PeakMaster (49.04 to 49.20 TU, where TU stands for Tiselius units, that is, 10^{-9} $m^2 \cdot V^{-1} \cdot s^{-1}$).[41] The

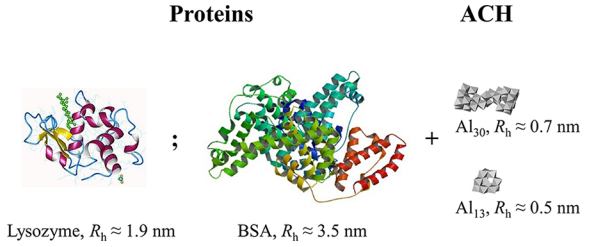

Figure 1. Schematic representation of the characteristic sizes of proteins (BSA and LSZ) and ACH constituents. R_h stands for the hydrodynamic radius. Values can be found in the literature for BSA and LSZ[43] and were calculated using a cylindrical model for Al_{13} and Al_{30}.[44]

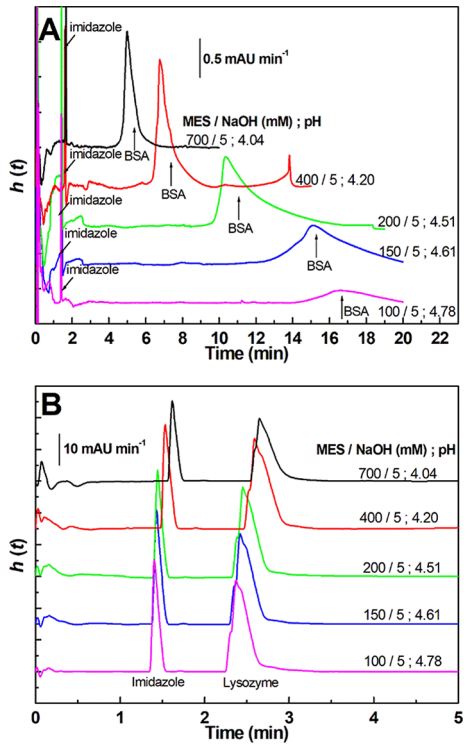

Figure 2. Electropherograms of (A) BSA and (B) LSZ at different pH values in MES−Na electrolytes. Electrophoretic conditions: UltraTol LN coating on a silica capillary with 50 μm i.d. × 38.5 cm (effective length, 30 cm). Electrolyte: 5 mM NaOH and X mM MES as indicated on the graph. Applied voltage: +30 kV (5−7 μA). Hydrodynamic injection: 50 mbar, 5 s. Indirect UV detection at 205 nm. Samples: 2.0 g/L BSA, 0.5 g/L Im in H_2O; 2.0 g/L LSZ and 0.5 g/L Im in H_2O. Im is used as a mobility marker. $h(t)$ is the absorbance divided by the migration time, which represents a mass-weighted distribution of the migration time.[45]

migration times of LSZ (pI 9.3) are much shorter than those of BSA (pI 4.7) because of higher protonation and, thus, a higher effective mobility. Figure 3A plots changes in the effective electrophoretic mobility of both proteins ($n = 4$ repetitions) as a function of pH, with the error bars representing the peak dispersion (with typical min/max mobilities obtained using eq 3 by peak integration). Both proteins are positively charged in the investigated range of pH values. As expected, the effective mobility of the LSZ is about 30 TU and remains constant over the pH range explored in this work. On the contrary, the effective mobility of the more acidic BSA decreases when the pH increases and approaches the pI value (4.7).

DOI: 10.1021/acsomega.8b02326
ACS Omega 2018, 3, 17547−17554

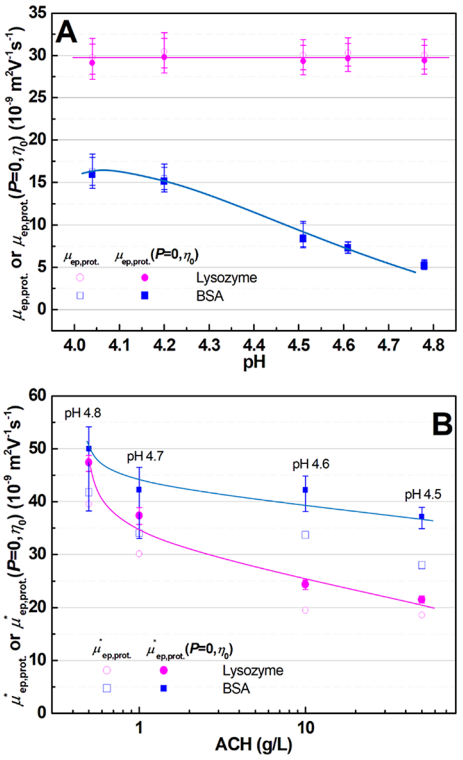

Figure 3. Evolution of the effective electrophoretic mobility of LSZ and BSA at (A) different pH in absence of ACH and (B) different ACH concentrations. Electrophoretic conditions as in Figure 2 (in the absence of ACH) or as in Figure 4 (in the presence of ACH).

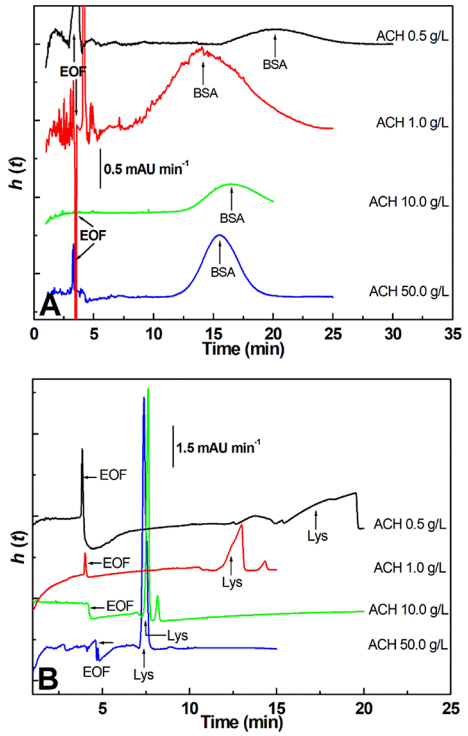

Figure 4. Electropherograms of (A) BSA and (B) LSZ at different ACH concentrations. Electrophoretic conditions: UltraTol LN coating on silica capillary 50 μm i.d. × 38.5 cm (effective length, 30 cm). Electrolyte: X g/L ACH as indicated on the graph, no other buffer additives. Applied voltage: −10 kV. Hydrodynamic injection: 50 mbar, 5 s. Indirect UV detection at 205 nm. Samples: 2.0 g/L BSA, 0.5 g/L Im in H_2O; 2.0 g/L LSZ, 0.5 g/L Im in H_2O.

Figure 4 presents the electropherograms obtained by injection of the protein (BSA or LSZ, dissolved in water) using ACH as a BGE (without any other additives), at different ACH concentrations from 0.5 up to 50 g/L at −10 kV. This way, the electrophoretic experiment mimics the interactions occurring when the proteins are put into contact with the ACH antiperspirant ingredients. The ACH used in this work contained 9.6% Al_{13} to Al_{13} + Al_{30} mass proportion, as previously quantified.[14] Despite the use of a neutral coating, the electroosmotic flow is reversed (μ_{eo} was between −57.7 and −65.4 TU) in the presence of ACH, because of the adsorption of ACH cationic oligomers onto the capillary surface. Also, the applied voltage absolute value is reduced to −10 kV (compared to +30 kV in the absence of ACH) to limit Joule heating. Despite the decrease of the applied voltage, the current intensity varied from 8.7 μA at 0.5 g/L up to 147.5 μA at 50 g/L as given in Table 1 with other physicochemical characteristics of the ACH BGE, including pH, viscosity, dissipated power per capillary length, and the estimated BGE ionic strength.

To extract information about protein−ACH interactions from the effective mobilities of the proteins, it is crucial to correct the experimental values from different important effects: Joule heating, BGE viscosity, fluctuation of ionization state with pH, and the ionic strength effect.

3.2. Correction from Joule Heating Effect. Although the CE apparatus enables precise control of the temperature of the cassette by air cooling, the equilibrium temperature (T) inside the capillary during the electrophoretic migration is always different from the temperature setpoint (T_{set}). The difference in temperature $\delta T = T - T_{set}$ can be estimated from the variation of conductivity at different dissipated power per capillary length (P/L).[46] For that, the dissipated power P obtained for NaCl solutions at different concentrations and for different applied voltages from +5 to +30 kV was recorded at T_{set} = 25 °C. The actual electric conductivity $\kappa(P)$ within the capillary, at a given dissipated power P, can be determined by eq 4

$$\kappa(P) = \frac{PL}{V^2 S} \tag{4}$$

where V is the applied voltage and S is the capillary cross section. The relative variation of the conductivity, which is similar to the relative variation of mobility, can be linearized for P/L lower than 4 W/m according to eq 5

$$\left[\frac{\kappa(P)}{\kappa(P=0)}\right]_{T_{set}} = \left[\frac{\mu_{ep,prot}(P)}{\mu_{ep,prot}(P=0)}\right]_{T_{set}} = \left[1 + \alpha\frac{P}{L}\right]_{T_{set}} \tag{5}$$

where α is a parameter that is a characteristic of the thermoregulation of a CE apparatus at a given T_{set}. Figure SI1A in Supporting Information displays the correlation between the conductivity ratio and the P/L value, leading to the determination of an α parameter for an Agilent G7100 apparatus at a specific temperature setpoint of 25 °C (α = 0.0507). Thus, the effective mobility corrected from Joule heating effect can be obtained by:[46]

$$\mu_{ep,prot}(P=0) = \frac{\mu_{ep,prot}(P)}{1 + \alpha\frac{P}{L}} \tag{6}$$

DOI: 10.1021/acsomega.8b02326
ACS Omega 2018, 3, 17547−17554

Please note that eq 5 is valid in the absence ($\mu_{ep,prot}$) or in the presence ($\mu^*_{ep,prot}$) of ACH. Equation 6 provides a temperature-related mobility correction, but the elevation in temperature δT within the capillary remains unknown. Besides this mobility correction, the measured value of the α parameter (eq 5) can be utilized for an estimation of the elevation in temperature δT using eq 7[46]

$$\delta T = \frac{\alpha}{\Theta}\frac{P}{L} \tag{7}$$

with

$$\Theta = -\frac{1}{\eta_{(P=0)}}\left(\frac{d\eta}{dT}\right)_{T_{set}} \tag{8}$$

where Θ is a parameter depending only on the variation of viscosity of the solvent (BGE) and $\eta_{(P=0)}$ is the viscosity of the BGE at T_{set}. Θ values and the corresponding δT are gathered in Table 1 for various BGEs. The elevation of temperature within the capillary is negligible in the MES/NaOH BGE and goes from +0.3 °C at 0.5 g/L ACH to +2.2 °C at 10 g/L ACH and up to +12.7 °C at 50.0 g/L ACH (see Table 1). Lower applied voltage would be required to reduce this elevation of temperature, but the analysis time (about 30 min at −10 kV for BSA) would also be increased.

3.3. Correction for the Viscosity of the BGE. Apart from the equilibrium temperature within the capillary, the viscosity of the BGE significantly increases with ACH concentration (from 1.07 cP at 0.5 g/L up to 1.34 at 50 g/L; see Table 1). To correct for the viscosity effect, the electrophoretic mobility of the protein was normalized to the viscosity of water (η_0 = 0.89 cP) using eq 9:

$$\mu_{ep,prot}(P=0,\eta_0) = \mu_{ep,prot}(P=0)\times\frac{\eta}{\eta_0} \tag{9}$$

The viscosity- and Joule heating-corrected mobilities, $\mu^*_{ep,prot}(P=0,\eta_0)$, are displayed in Figure 3. Clearly, in the absence of ACH (Figure 3A), the corrections are negligible (open vs plain symbols), whereas in the presence of ACH (Figure 3B), mobility corrections from 2 up to 9 TU could be observed. It is worth noting that in the difference observed between $\mu^*_{ep,prot}$ and $\mu^*_{ep,prot}(P=0,\eta_0)$, the viscosity correction and the Joule heating correction partially vanish.

3.4. Correction for the Ionization State of the Protein. In the case of LSZ, the change in pH of the BGE with ACH concentration does not impact the ionization state of the protein because the investigated range of pH values (4.0−4.8) is far from the pI. On the contrary, the ionization state of BSA strongly changes with the concentration of ACH. It was thus necessary to correct for this effect. Accordingly, the ratio R was introduced, defined as the ratio of the viscosity- and Joule heating-corrected effective mobilities in the presence of ACH, $\mu^*_{ep,prot}(P=0,\eta_0)$, and in the absence of ACH at 5 mM ionic strength, $\mu^{5\,mM}_{ep,prot}(P=0,\eta_0)$, for a given pH:

$$R = \left[\frac{\mu^*_{ep,prot}(P=0,\eta_0)}{\mu^{5mM}_{ep,prot}(P=0,\eta_0)}\right]_{pH} \tag{10}$$

This definition of the R parameter is still ionic strength dependent, and we will comment on it later. R = 1 means that there is no interaction between the protein and the ACH species. An R value higher than 1 is expected if the interaction between the protein and the ACH would increase the positive charge of the protein, and thus, its effective mobility. R is expected to be an increasing function of the binding constant between the ligand(s) and the receptor as far as the ligand(s) speeds up the receptor, but R increases also with increasing mobility of the complex. R < 1 could be observed if the interaction between the protein and the metal cation leads to a decrease in the global charge of the protein and/or to a change in conformation leading to a decrease in effective mobility. Such an effect was observed by Wätzig et al. by classical ACE for BSA and barium interactions (at 250 μM $BaCl_2$, in a 20 mM TRIS BGE, and pH 7.4).[39] In this study, R < 1 could be also caused by the increase of the ionic strength when the ACH concentration increases. Indeed, it is a very general trend in electrophoresis that for any solutes (small ion, polyelectrolyte, proteins, and nanoparticles), the effective mobility is a decreasing function of the ionic strength.[43,47,48]

Figure 5A displays the mobility ratio R as a function of ACH concentration. Clearly, the R values are much higher for BSA

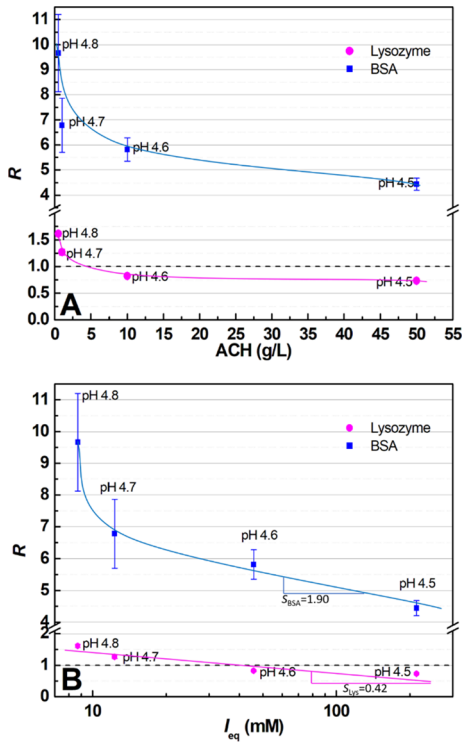

Figure 5. Variation of the mobility ratio R as a function of (A) ACH concentration and as a function of (B) ionic strength. Electrophoretic conditions as in Figure 2 (in the absence of ACH) and Figure 4 (in the presence of ACH).

(typically between 4.4 and 9.7) than for LSZ (0.7 to 1.6) suggesting much higher interaction of BSA with ACH compared to LSZ. These results are in very good agreement with those obtained by Deschaume et al.[17] by FTIR, showing strong electrostatic interactions between ACH and BSA involving acidic groups (Asp and Glu) and weaker interactions between ACH and LSZ based on hydrogen bonding. This is quite intuitive if one considers the global high positive charge of LSZ, as compared to BSA, which should be more electrostatically repulsive against the ACH ligands. Nevertheless and surprisingly, even for LSZ, R values up to 1.6 were observed, which demonstrates that interactions are also

DOI: 10.1021/acsomega.8b02326
ACS Omega 2018, 3, 17547−17554

present, to a lower extent. For LSZ, the R value drops below 1 above 10 g/L ACH. The dependence of R with the ionic strength is discussed in the next section.

3.5. Estimation of the Influence of the Ionic Strength of the BGE on R Values. Figure 5B displays the mobility ratio, R, as a function of the (estimated) ionic strength of the ACH solutions on a semilogarithmic scale. It is impossible to know the exact ionic strength of the ACH solutions because of the complexity of the oligomeric mixtures. However, a rough estimation of the ionic strength can be obtained from the current intensities. The equivalent ionic strength I_{eq} of the ACH BGE was estimated from the NaCl concentration leading to the same current intensity under the same electrophoretic conditions (−10 kV, same capillary dimensions). The I_{eq} values are given in Table 1 and vary between 8.7 mM at 0.5 g/L and 213 mM at 50 g/L. It is worth noting that the Na^+ ion has a similar effective mobility to Al_{13} and Al_{30} oligomers,[14] and Cl^- is the natural counterion for ACH.

The S parameter, which has been recently introduced in the so-called slope plot approach,[14,47−50] is a quantitative non-dimensional parameter that characterizes the amplitude of the decrease in effective mobility with the ionic strength. The slope of the decrease of the R ratio on a semilogarithmic scale, as presented in Figure 5B, is about S_{LSZ} = 0.42 for LSZ, which is in good agreement with the typical S values obtained for proteins in acetate−NaCl electrolyte without metal ions.[43] The $R > 1$ at the low values of I_{eq} reveals an existing interaction between LSZ and ACH. Additionally, from the S_{LSZ} value, we can conclude that the interaction between LSZ and ACH remains stable regardless of the concentration of the ligand (ACH), because the decrease in the electrophoretic mobility of LSZ in the presence of ACH is only due to the ionic strength dependence. In the case of BSA, the mobility ratio, R, decreases much faster with increasing ACH concentration compared to LSZ. The slope of the linear part of the ionic strength dependence S_{BSA} = 1.90 is much too high to be only due to the ionic strength effect on the mobility. As a conclusion, it can be inferred that the interaction between BSA and ACH decreases with increasing ionic strength. Nevertheless, the R value remains very high (about 4.5) at I_{eq} = 213 mM (i.e., at 50 g/L ACH), meaning that the BSA−ACH interaction is still very strong.

4. CONCLUSIONS

In this work, it has been demonstrated that it is possible to study and quantify the interactions between proteins (receptor) and ACH (ligands) by ACE using high concentrations of ligands (0.5−50 g/L in ACH) and no buffering additive in the BGE. Such an approach is very different from classical ACE, where the ligand is generally introduced in the BGE with a buffering component that set the pH. In this work, the ligand mixture itself (ACH) was used as a BGE, to mimic as much as possible the conditions of industrial applications. To extract the information about the interaction, it is however important to take into account the different parameters that vary with the ACH concentration and change the protein mobility: Joule heating, viscosity, protein protonation, and ionic strength. The ratio R of the corrected effective mobility of the protein in the presence of ACH (ligand) relative to the corrected effective mobility of the protein in the absence of ACH at the same pH and at 5 mM ionic strength was proposed as an estimator of the interaction. With relevant corrections on the effective mobility, it has been possible to identify two very different behaviors for the interaction of proteins with ACH. On the one hand, a strong interaction was observed between BSA and ACH, starting from low ACH concentration and decreasing in strength with increasing ACH concentration. On the other hand, a much weaker interaction between Lys and ACH was observed and remained stable regardless of the ACH concentration. As a perspective, it would be interesting to study the impact of formulation excipients (calcium or glycine, for instance) in the BGE on the protein−ACH interaction. The application of this approach to the study of ACH interaction with more specific sweat proteins, such as mucins, would be also relevant for the development of new antiperspirant products.

■ ASSOCIATED CONTENT

Supporting Information

The Supporting Information is available free of charge on the ACS Publications website at DOI: 10.1021/acsomega.8b02326.

Evaluation of the Joule heating parameter of Agilent 7100 CE apparatus (PDF)

■ AUTHOR INFORMATION

Corresponding Author

*E-mail: herve.cottet@umontpellier.fr. Tel: +33 4 67 14 34 27. Fax: +33 4 67 63 10 46.

ORCID

Hervé Cottet: 0000-0002-6876-175X

Notes

The authors declare no competing financial interest.

■ ACKNOWLEDGMENTS

We gratefully acknowledge Dr. V. Manzin and Dr. J.-B. Galey from L'Oréal Research & Innovation for fruitful discussions. N.O. and H.C. gratefully acknowledge the financial support from L'Oréal. H.C. and P.D. thank the bilateral PHC Barrande program no. 38094QC/Czech MOBILITY no. 7AMB17.

■ REFERENCES

(1) Teagarden, D. L.; Hem, S. L.; White, J. L. Conversion of Aluminum Chlorohydrate to Aluminum Hydroxide. *J. Soc. Cosmet. Chem* **1982**, *33*, 281−295.

(2) Brosset, C. On the Reactions of Aluminium Ion with Water. *Acta Chem. Scand.* **1952**, *6*, 910−940.

(3) Brosset, C.; Biedermann, G.; Sillén, L. G.; Sörensen, N. A. Studies on the Hydrolysis of Metal Ions. XI. The Aluminium Ion, Al^{3+}. *Acta Chem. Scand.* **1954**, *8*, 1917−1926.

(4) Sillén, L. G. On Equilibria in Systems with Polynuclear Complex Formation. I. Methods of Deducing the Composition of the Complexes from Experimental Data. "Core + Links" Complexes. *Acta Chem. Scand.* **1954**, *8*, 299−317.

(5) Stol, R. J.; Van Helden, A. K.; De Bruyn, P. L. Hydrolysis-Precipitation Studies of Aluminum (III) Solutions. 2. A Kinetic Study and Model. *J. Colloid Interface Sci.* **1976**, *57*, 115−131.

(6) Bretagne, A.; Cotot, F.; Arnaud-Roux, M.; Sztucki, M.; Cabane, B.; Galey, J.-B. The Mechanism of Eccrine Sweat Pore Plugging by Aluminium Salts Using Microfluidics Combined with Small Angle X-ray Scattering. *Soft Matter* **2017**, *13*, 3812−3821.

(7) Chen, X.; Gasecka, P.; Formanek, F.; Galey, J.-B.; Rigneault, H. *In Vivo* Single Human Sweat Gland Activity Monitoring Using Coherent Anti-Stokes Raman Scattering and Two-Photon Excited Autofluorescence Microscopy. *Br. J. Dermatol.* **2016**, *174*, 803−812.

(8) Rowsell, J.; Nazar, L. F. Speciation and Thermal Transformation in Alumina Sols: Structures of the Polyhydroxyoxoaluminum Cluster

DOI: 10.1021/acsomega.8b02326
ACS Omega 2018, 3, 17547−17554

$[Al_{30}O_8(OH)_{56}(H2O)_{26}]^{18+}$ and Its δ-Keggin Moieté. *J. Am. Chem. Soc.* **2000**, *122*, 3777−3778.
(9) Allouche, L.; Gérardin, C.; Loiseau, T.; Férey, G.; Taulelle, F. Al_{30}: A Giant Aluminum Polycation. *Angew. Chem., Int. Ed.* **2000**, *39*, 511−514.
(10) Allouche, L.; Taulelle, F. Conversion of Al_{13} Keggin ε into Al_{30}: A Reaction Controlled by Aluminum Monomers. *Inorg. Chem. Commun.* **2003**, *6*, 1167−1170.
(11) Williams, D. F.; Schmidtt, W. H., Eds. *Chemistry and Technology of the Cosmetics and Toiletries Industry*, 2nd ed; Blackie Academic: London, 1996.
(12) Fitzgerald, J. J.; Rosenberg, A. H. Chemistry of Aluminum Chlorohydrate and Activated Chlorohydrates. In *Antiperspirants and Deodorants*; Laden, K., Ed.; Marcel Dekker: New York, 1999; 83−136.
(13) Callaghan, D. T.; Phipps, A. M.; Provancal, S. J. Antiperspirant Composition. U.S. Patent 4,775,528, 1988.
(14) Ouadah, N.; Moire, C.; Kuntz, J.-F.; Brothier, F.; Cottet, H. Analysis and Characterization of Aluminum Chlorohydrate Oligocations by Capillary Electrophoresis. *J. Chromatogr. A* **2017**, *1492*, 144−150.
(15) Yuan, S.; Vaughn, J. S.; Pappas, I.; Fitzgerald, M.; Masters, J. G.; Pan, L. Optimal Aluminum/Zirconium: Protein Interactions for Predicting Antiperspirant Efficacy Using Zeta Potential Measurements. *J. Cosmet. Sci.* **2015**, *66*, 95−111.
(16) Deschaume, O.; Shafran, K. L.; Perry, C. C. Interactions of Bovine Serum Albumin with Aluminum Polyoxocations and Aluminum Hydroxide. *Langmuir* **2006**, *22*, 10078−10088.
(17) Deschaume, O.; Fournier, A.; Shafran, K. L.; Perry, C. C. Interactions of Aluminium Hydrolytic Species with Biomolecules. *New J. Chem.* **2008**, *32*, 1346.
(18) Rundlett, K. L.; Armstrong, D. W. Methods for the Determination of Binding Constants by Capillary Electrophoresis. *Electrophoresis* **2001**, *22*, 1419−1427.
(19) Busch, M. H. A; Kraak, J. C.; Poppe, H. Principles and Limitations of Methods Available for the Determination of Binding Constants with Affinity Capillary Electrophoresis. *J. Chromatogr. A* **1997**, *777*, 329−353.
(20) El Deeb, S.; Wätzig, H.; El-Hady, D. A.; Sänger-van de Griend, C.; Scriba, G. K. E. Recent Advances in Capillary Electrophoretic Migration Techniques for Pharmaceutical Analysis (2013−2015). *Electrophoresis* **2016**, *37*, 1591−1608.
(21) Heegaard, N. H. H.; Nissen, M. H.; Chen, D. D. Y. Applications of On-Line Weak Affinity Interactions in Free Solution Capillary Electrophoresis. *Electrophoresis* **2002**, *23*, 815−822.
(22) He, X.; Ding, Y.; Li, D.; Lin, B. Recent Advances in the Study of Biomolecular Interactions by Capillary Electrophoresis. *Electrophoresis* **2004**, *25*, 697−711.
(23) Gao, J. Y.; Dubin, P. L.; Muhoberac, B. B. Measurement of the Binding of Proteins to Polyelectrolytes by Frontal Analysis Continuous Capillary Electrophoresis. *Anal. Chem.* **1997**, *69*, 2945−2951.
(24) Hattori, T.; Kimura, K.; Seyrek, E.; Dubin, P. L. Binding of Bovine Serum Albumin to Heparin Determined by Turbidimetric Titration and Frontal Analysis Continuous Capillary Electrophoresis. *Anal. Biochem.* **2001**, *295*, 158−167.
(25) Hattori, T.; Hallberg, R.; Dubin, P. L. Roles of Electrostatic Interaction and Polymer Structure in the Binding of β-Lactoglobulin to Anionic Polyelectroytes: Measurement of Binding Constants by Frontal Analysis Continuous Capillary Electrophoresis. *Langmuir* **2000**, *16*, 9738−9743.
(26) Sisavath, N.; Leclercq, L.; Le Saux, T.; Oukacine, F.; Cottet, H. Study of Interactions between Oppositely Charged Dendrigraft Poly-L-Lysine and Human Serum Albumin by Continuous Frontal Analysis Capillary Electrophoresis and Fluorescence Spectroscopy. *J. Chromatogr. A* **2013**, *1289*, 127−132.
(27) Lounis, F. M.; Chamieh, J.; Leclercq, L.; Gonzalez, P.; Cottet, H. The Effect of Molar Mass and Charge Density on the Formation of Complexes between Oppositely Charged Polyelectrolytes. *Polymers* **2017**, *9*, 50.
(28) Gomez, F. A.; Avila, L. Z.; Chu, Y.-H.; Whitesides, G. M. Determination of Binding Constants of Ligands to Proteins by Affinity Capillary Electrophoresis: Compensation for Electroosmotic Flow. *Anal. Chem.* **1994**, *66*, 1785−1791.
(29) Mito, E.; Gomez, F. A. Flow-through Partial-Filling Affinity Capillary Electrophoresis for the Estimation of Binding Constants of Ligands to Receptors. *Chromatographia* **1999**, *50*, 689−694.
(30) Heintz, J.; Hernandez, M.; Gomez, F. A. Use of a Partial-Filling Technique in Affinity Capillary Electrophoresis for Determining Binding Constants of Ligands to Receptors. *J. Chromatogr. A* **1999**, *840*, 261−268.
(31) Zhang, W.; Zhang, L.; Ping, G.; Zhang, Y.; Kettrup, A. Study on the Multiple Sites Binding of Human Serum Albumin and Porphyrin by Affinity Capillary Electrophoresis. *J. Chromatogr. B* **2002**, *768*, 211−214.
(32) Anderot, M.; Nilsson, M.; Végvári, Á.; Moeller, E. H.; van de Weert, M.; Isaksson, R. Determination of Dissociation Constants between Polyelectrolytes and Proteins by Affinity Capillary Electrophoresis. *J. Chromatogr. B* **2009**, *877*, 892−896.
(33) Müllerová, L.; Dubský, P.; Gaš, B. Generalized Model of Electromigration with 1:1 (Analyte:Selector) Complexation Stoichiometry: Part II. Application to Dual Systems and Experimental Verification. *J. Chromatogr. A* **2015**, *1384*, 147−154.
(34) Dubský, P.; Dvořák, M.; Ansorge, M. Affinity Capillary Electrophoresis: The Theory of Electromigration. *Anal. Bioanal. Chem.* **2016**, *408*, 8623−8641.
(35) Šolínová, V.; Mikysková, H.; Kaiser, M. M.; Janeba, Z.; Holý, A.; Kašička, V. Estimation of Apparent Binding Constant of Complexes of Selected Acyclic Nucleoside Phosphonates with β-Cyclodextrin by Affinity Capillary Electrophoresis. *Electrophoresis* **2016**, *37*, 239−247.
(36) Redweik, S.; Xu, Y.; Wätzig, H. Precise, Fast, and Flexible Determination of Protein Interactions by Affinity Capillary Electrophoresis: Part 1: Performance. *Electrophoresis* **2012**, *33*, 3316−3322.
(37) Redweik, S.; Cianciulli, C.; Hara, M.; Xu, Y.; Wätzig, H. Precise, Fast and Flexible Determination of Protein Interactions by Affinity Capillary Electrophoresis. Part 2: Cations. *Electrophoresis* **2013**, *34*, 1812−1819.
(38) Xu, Y.; Redweik, S.; El-Hady, D. A.; Albishri, H. M.; Preu, L.; Wätzig, H. Precise, Fast, and Flexible Determination of Protein Interactions by Affinity Capillary Electrophoresis: Part 3: Anions. *Electrophoresis* **2014**, *35*, 2203−2212.
(39) Alhazmi, H. A.; Nachbar, M.; Albishri, H. M.; El-Hady, D. A.; Redweik, S.; El Deeb, S.; Wätzig, H. A Comprehensive Platform to Investigate Protein−Metal Ion Interactions by Affinity Capillary Electrophoresis. *J. Pharm. Biomed. Anal.* **2015**, *107*, 311−317.
(40) Ehala, S.; Toman, P.; Rathore, R.; Makrlík, E.; Kašička, V. Affinity Capillary Electrophoresis and Quantum Mechanical Calculations Applied to the Investigation of Hexaarylbenzene-Based Receptor Binding with Lithium Ion. *J. Sep. Sci.* **2011**, *34*, 2433−2440.
(41) Gaš, B.; Jaroš, M.; Hruška, V.; Zusková, I.; Štedrý, M. PeakMaster - A Freeware Simulator of Capillary Zone Electrophoresis. *LC GC Eur.* **2005**, *18*, 282−288.
(42) Dubský, P.; Ördögová, M.; Malý, M.; Riesová, M. CEval: All-in-One Software for Data Processing and Statistical Evaluations in Affinity Capillary Electrophoresis. *J. Chromatogr. A* **2016**, *1445*, 158−165.
(43) Bekri, S.; Leclercq, L.; Cottet, H. Influence of the Ionic Strength of Acidic Background Electrolytes on the Separation of Proteins by Capillary Electrophoresis. *J. Chromatogr. A* **2016**, *1432*, 145−151.
(44) Deschamps, J.; Dutremez, S. G.; Boury, B.; Cottet, H. Size-Based Characterization of an Ionic Polydiacetylene by Taylor Dispersion Analysis and Capillary Electrophoresis. *Macromolecules* **2009**, *42*, 2679−2685.
(45) Chamieh, J.; Martin, M.; Cottet, H. Quantitative Analysis in Capillary Electrophoresis: Transformation of Raw Electropherograms into Continuous Distributions. *Anal. Chem.* **2015**, *87*, 1050−1057.

DOI: 10.1021/acsomega.8b02326
ACS Omega 2018, 3, 17547−17554

(46) Plasson, R.; Cottet, H. Determination of Homopolypeptide Conformational Changes by the Modeling of Electrophoretic Mobilities. *Anal. Chem.* **2005**, *77*, 6047−6054.
(47) Ibrahim, A.; Meyrueix, R.; Pouliquen, G.; Chan, Y. P.; Cottet, H. Size and Charge Characterization of Polymeric Drug Delivery Systems by Taylor Dispersion Analysis and Capillary Electrophoresis. *Anal. Bioanal. Chem.* **2013**, *405*, 5369−5379.
(48) Cottet, H.; Wu, H.; Allison, S. A. On the Ionic Strength Dependence of the Electrophoretic Mobility: From 2D to 3D Slope-Plots. *Electrophoresis* **2017**, *38*, 624−632.
(49) Bekri, S.; Leclercq, L.; Cottet, H. Polyelectrolyte Multilayer Coatings for the Separation of Proteins by Capillary Electrophoresis: Influence of Polyelectrolyte Nature and Multilayer Crosslinking. *J. Chromatogr. A* **2015**, *1399*, 80−87.
(50) Ibrahim, A.; Koval, D.; Kašička, V.; Faye, C.; Cottet, H. Effective Charge Determination of Dendrigraft Poly-L-Lysine by Capillary Isotachophoresis. *Macromolecules* **2013**, *46*, 533−540.

DOI: 10.1021/acsomega.8b02326
ACS Omega 2018, 3, 17547−17554